
WAIM-Based Dual-Polarized Antenna Synthesis for 5G Base Station

G. Oliveri, M. Salucci and A. Massa

Contents

1	Numerical Results	3
1.1	WAIM Optimization [$Q = 8$]	3
1.1.1	PSO [$Q = 8, K = 9, P = 8, I = 50$]	3

ELEDIA Research Center

1 Numerical Results

1.1 WAIM Optimization [$Q = 8$]

1.1.1 PSO [$Q = 8, K = 9, P = 8, I = 50$]

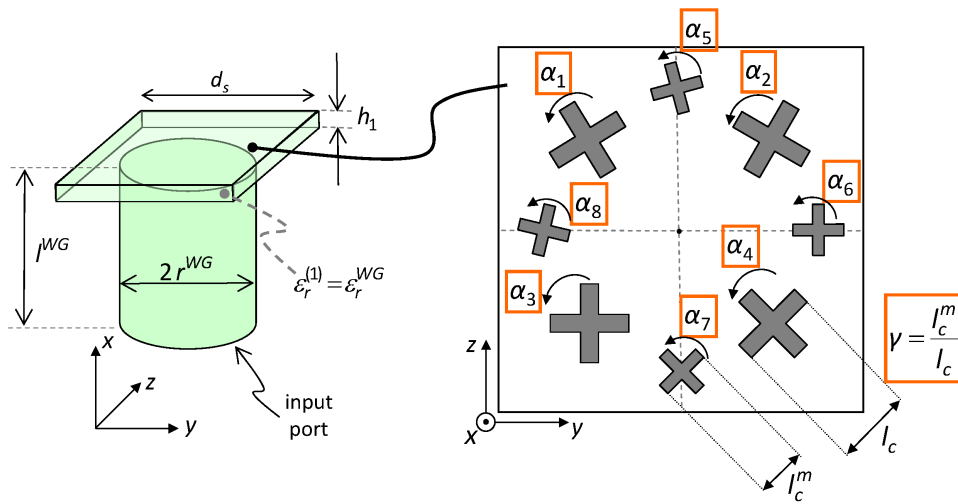
Find a configuration of the WAIM able to minimize the scan loss with eight symmetrical crosses as metallizations. Some of the parameters such as l_c, w_c, d_c, h_1 are preserved from the best solution with $Q = 4$ (III). The DoFs are the angles of the added four crosses which are free and the scaling with respect to the previous crosses. These should enable higher performance and the symmetry should again preserve the array behaviour in steering and between the modes/polarizations

DoFs

- Number of variables, $K = 9$
- Number of WAIM crosses, $Q = 8$
- Optimization variables and ranges

Physical Meaning	Variable	min	max
Tilt of upper left cross	α_1	0 [deg]	90 [deg]
Tilt of upper right cross	α_2	0 [deg]	90 [deg]
Tilt of lower left cross	α_3	0 [deg]	90 [deg]
Tilt of lower right cross	α_4	0 [deg]	90 [deg]
Tilt of secondary upper cross	α_5	0 [deg]	90 [deg]
Tilt of secondary left cross	α_6	0 [deg]	90 [deg]
Tilt of secondary right cross	α_7	0 [deg]	90 [deg]
Tilt of secondary lower cross	α_8	0 [deg]	90 [deg]
Scaling	γ	20 [%]	75 [%]

Table I: Variable ranges ($Q = 8, K = 9$) - Minimum and maximum allowed values.



(a)

Figure 1: WAIM ($Q = 8$) - Variable physical meaning on the WAIM geometry.

Optimization Parameters

- Optimization algorithm, *PSO*
- Number of particles, $P = 8$
- Number of iterations, $I = 50$
- Swarm initialization, *Random*
- Inertial weight, $w = 0.8$
- Acceleration coefficients, $C_1 = C_2 = 2.0$
- Random seed value, $s = 1$

Cost Function

- Angles considered, $N_a = 9$
 - $\phi \in \{-60, 0, 60\}$ [deg] $\times \theta \in \{75, 90, 105\}$ [deg]
- Frequencies considered, $N_f = 3$

- $f = \{3.30, 3.55, 3.80\}$ [GHz]

- Modes considered, $N_m = 2$ (± 45 [deg])
- S -parameter threshold, $S_{th} = -10$ [dB]

Results

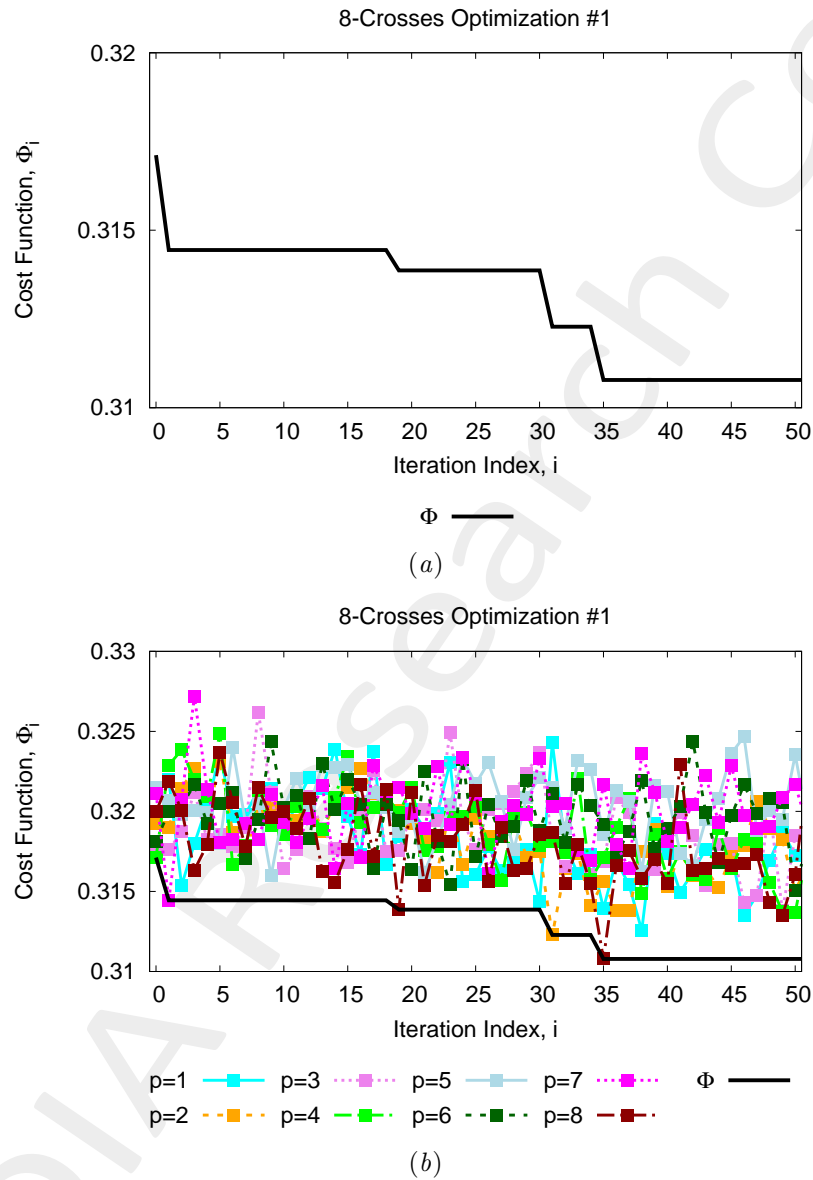


Figure 2: *Periodic model* ($Q = 8$, $s = 1$, $P = 8$, $I = 50$) - *PSO* Optimization. Cost vs iteration for (a) the global best solution of the *PSO* and (b) showing also the cost of all the *PSO* particles ($p = 1, \dots, 8$).

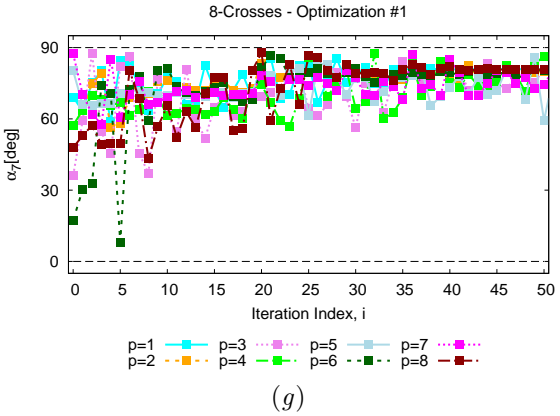
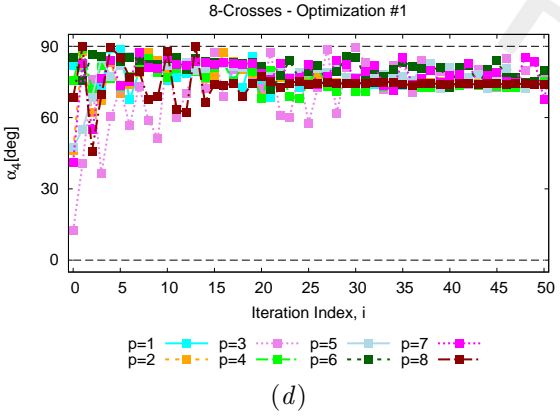
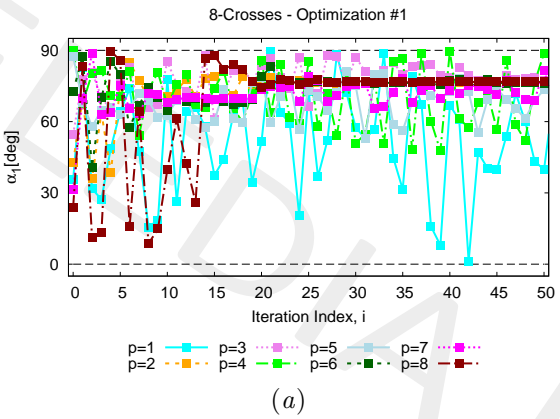
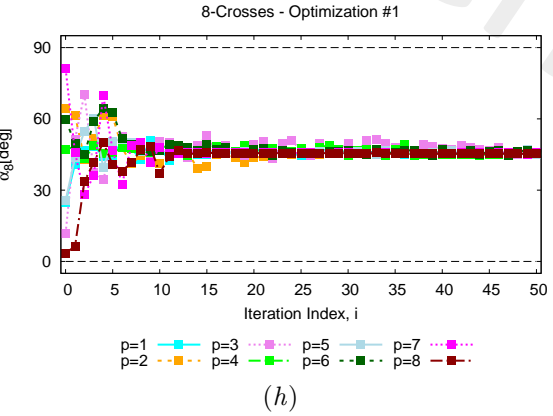
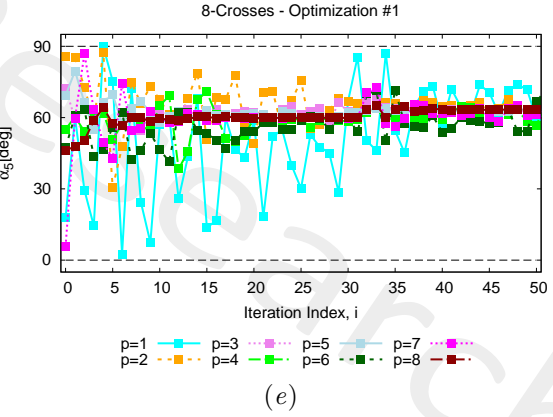
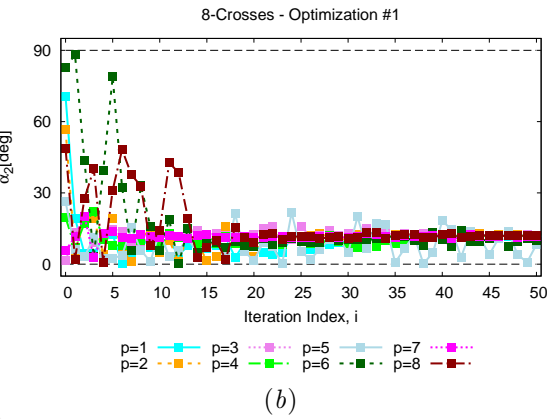
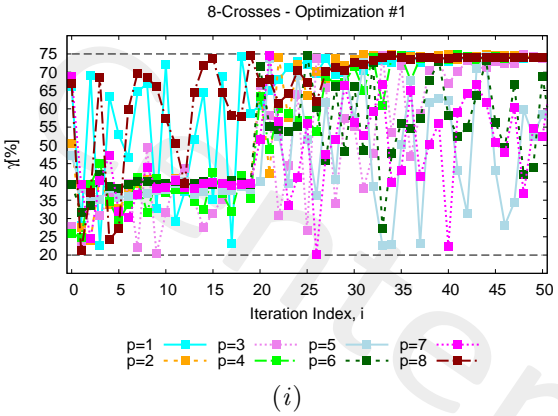
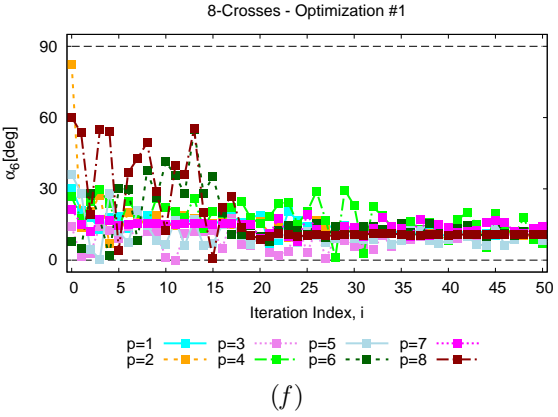
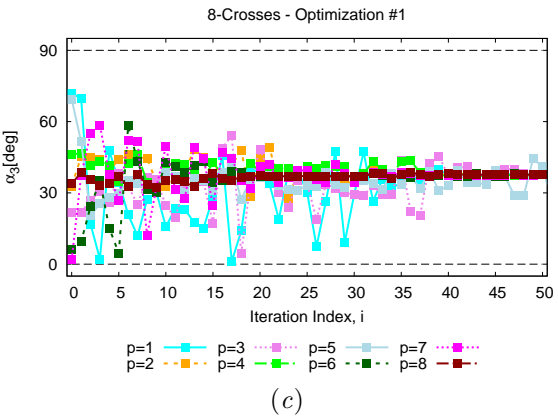
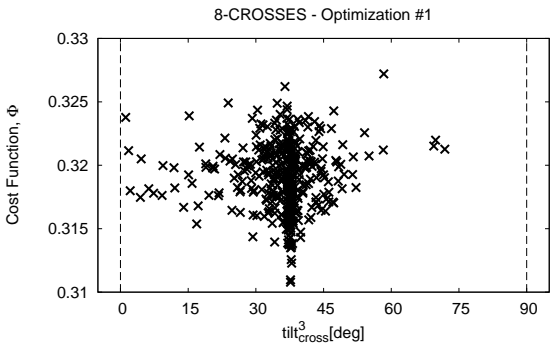
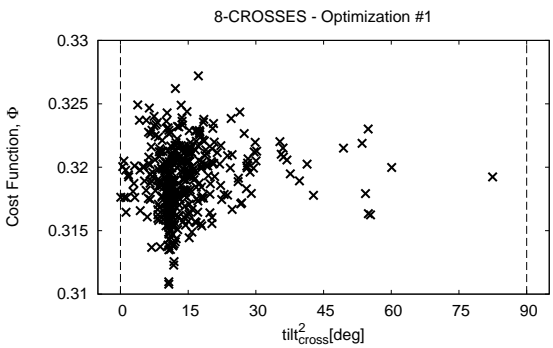


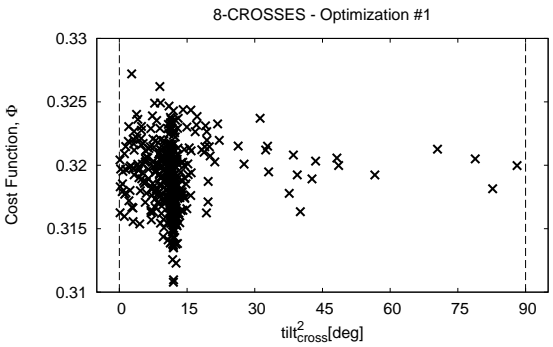
Figure 3: *Periodic model* ($Q = 8, s = 1, P = 8, I = 50$) - *PSO* Optimization. Variable vs iteration for all the *PSO* particles ($p = 1, \dots, 8$).



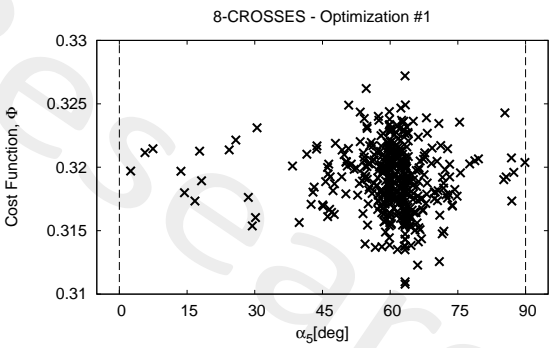
(c)



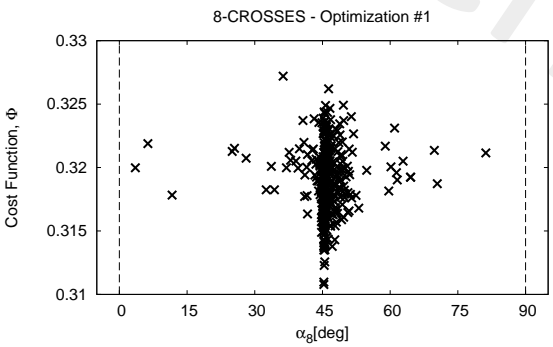
(i)



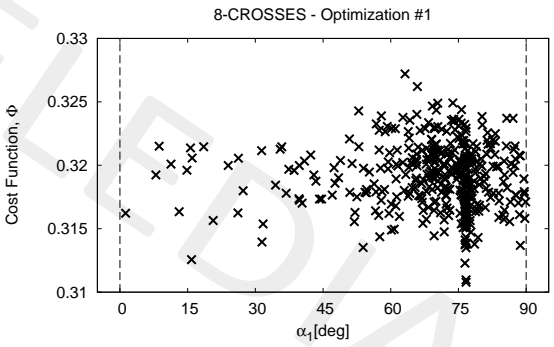
(b)



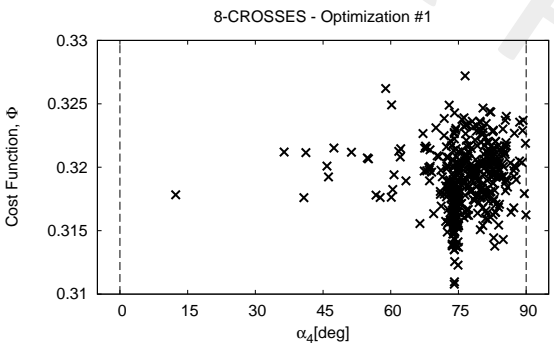
(e)



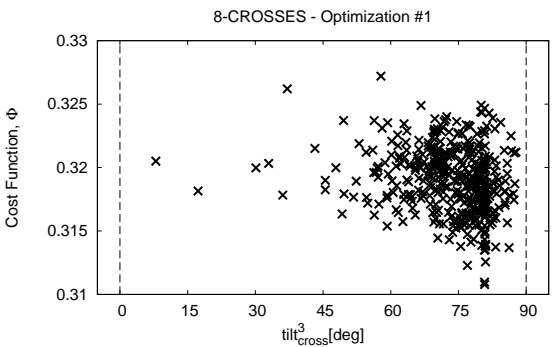
(h)



(a)



(d)



(g)

Figure 4: *Periodic model* ($Q = 8$, $s = 1$, $P = 8$, $I = 50$) - *PSO* Optimization. Cost vs variable for all the configurations simulated during the optimization.

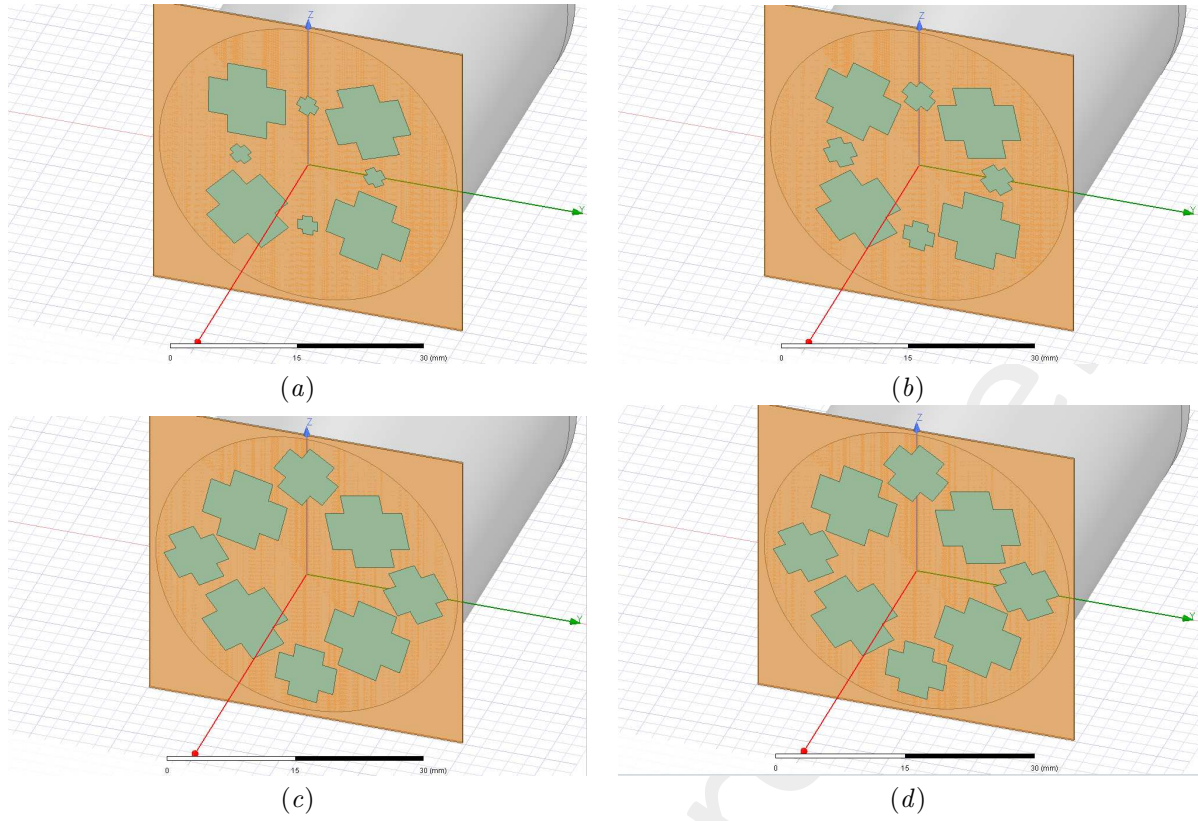


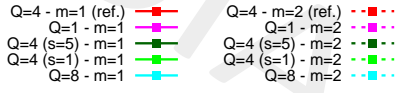
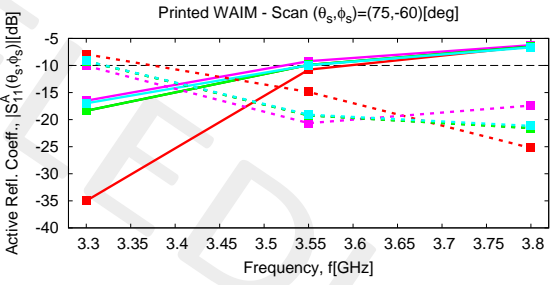
Figure 5: *Periodic model* ($Q = 8$, $s = 1$, $P = 8$, $I = 50$) - *PSO* Optimization. Best solution geometry at iterations (a) $i = 0$, (b) $i = 10$, (c) $i = 20$, (d) $i = 40$.

Iteration, i	Φ
0	3.171×10^{-1}
10	3.144×10^{-1}
20	3.139×10^{-1}
30	3.139×10^{-1}
40	3.108×10^{-1}
50	3.108×10^{-1}

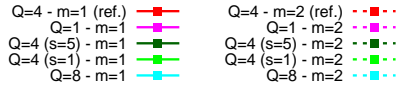
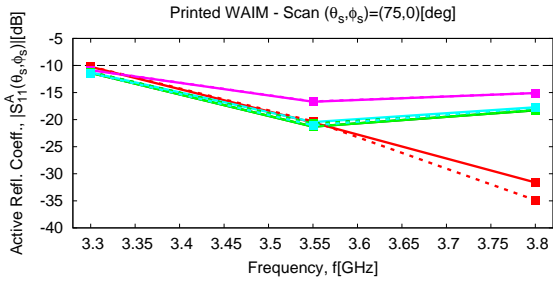
Table II: *Periodic model* ($Q = 8$, $s = 1$, $P = 8$, $I = 50$) - *PSO* Optimization. Cost function at the first iteration compared with the latest iteration. The first iterations represents a random sampling with $P = 8$ samples.

Physical Meaning	Variable	Value	$Q = 4$ $s = 1$ (Tab. III)
Length of the cross arms	l_c	9.836 [mm]	9.836 [mm]
Width of the cross arms	w_c	4.953 [mm]	4.953 [mm]
Distance of the cross centers from the FWG center	d_c	7.706 [mm]	7.706 [mm]
Superstrate thickness	h_1	0.245 [mm]	0.245 [mm]
Tilt of upper left cross	α_1	76.68 [deg]	12.70 [deg]
Tilt of upper right cross	α_2	11.96 [deg]	28.00 [deg]
Tilt of lower left cross	α_3	37.68 [deg]	27.65 [deg]
Tilt of lower right cross	α_4	74.07 [deg]	19.50 [deg]
Tilt of secondary upper cross	α_5	63.31 [deg]	/
Tilt of secondary left cross	α_6	10.70 [deg]	/
Tilt of secondary right cross	α_7	80.80 [deg]	/
Tilt of secondary lower cross	α_8	45.30 [deg]	/
Scaling	γ	73.9 [%]	/

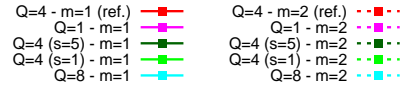
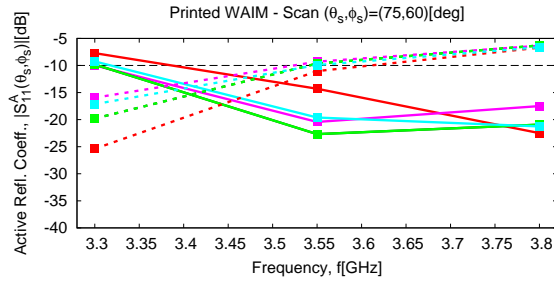
Table III: *Periodic model* ($Q = 8$, $s = 1$, $P = 8$, $I = 50$) - *PSO* Optimization. Parameter values of the best solution.



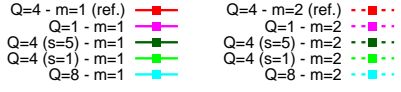
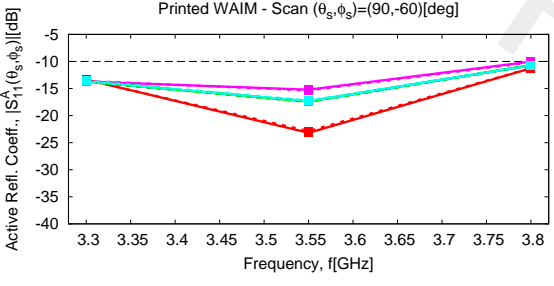
(a)



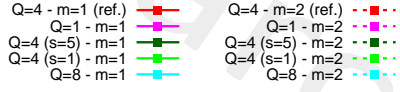
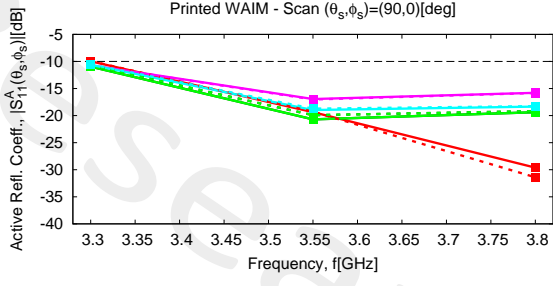
(b)



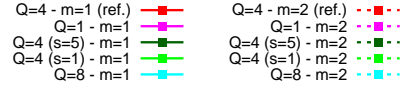
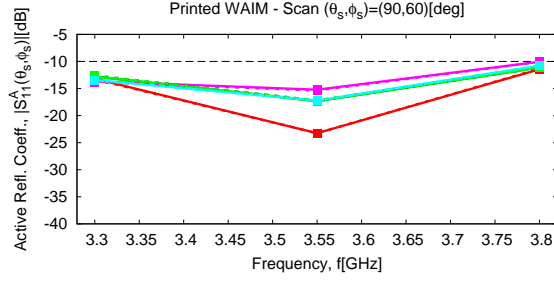
(c)



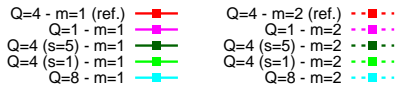
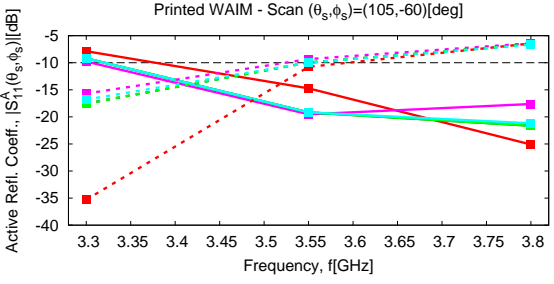
(d)



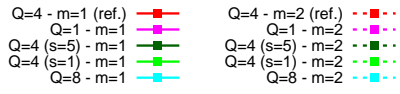
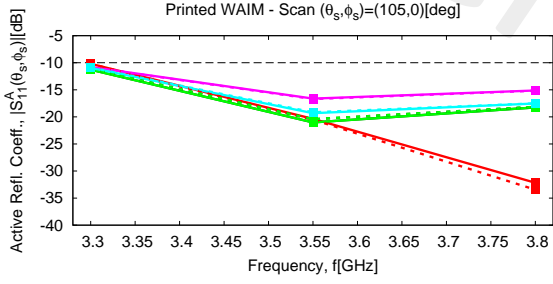
(e)



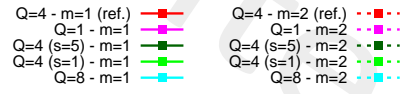
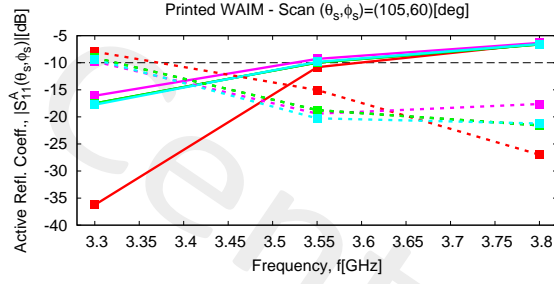
(f)



(g)



(h)



(i)

Figure 6: *Periodic model* ($Q = 8$, $s = 1$, $P = 8$, $I = 50$) - 5-parameter performance of best solution obtained with each $Q = 8$ compared with the previous setups ($Q = 1$, $Q = 4$), reported in the frequency range for the two polarizations ($m = 1, 2$) and in all the considered array scan points. The “Reference” solution, in red, comes from a previous optimization $Q = 4$ where the frequency range was $f \in [3.4, 3.8]$ [GHz]

Observations

- The dynamic of the cost function curve is very limited, probably due to the fixing of several parameters related to the four “base” crosses from a previous optimization.
- After just $i \simeq 10$ iterations the performance are better than the $Q = 4$ best solution.
- Overall the final solution improves only of 1.3% with respect to the best solution with $Q = 4$ crosses which is an almost negligible improvement as can be seen in Fig. 6.

More information on the topics of this document can be found in the following list of references.

References

- [1] M. Salucci, G. Oliveri, M. A. Hannan, and A. Massa, "System-by-design paradigm-based synthesis of complex systems: The case of spline-contoured 3D radomes," *IEEE Antennas and Propagation Magazine - Special Issue on 'Artificial Intelligence in Electromagnetics,'*, vol. 64, no. 1, pp. 72-83, Feb. 2022.
- [2] G. Oliveri, P. Rocca, M. Salucci, and A. Massa, "Holographic smart EM skins for advanced beam power shaping in next generation wireless environments," *IEEE J. Multiscale Multiphysics Comput. Tech.*, vol. 6, pp. 171-182, Oct. 2021.
- [3] G. Oliveri, A. Gelmini, A. Polo, N. Anselmi, and A. Massa, "System-by-design multi-scale synthesis of task-oriented reflectarrays," *IEEE Trans. Antennas Propag.*, vol. 68, no. 4, pp. 2867-2882, Apr. 2020.
- [4] M. Salucci, L. Tenuti, G. Gottardi, A. Hannan, and A. Massa, "System-by-design method for efficient linear array miniaturisation through low-complexity isotropic lenses" *Electronic Letters*, vol. 55, no. 8, pp. 433-434, May 2019.
- [5] M. Salucci, N. Anselmi, S. Goudos, and A. Massa, "Fast design of multiband fractal antennas through a system-by-design approach for NB-IoT applications" *EURASIP J. Wirel. Commun. Netw.*, vol. 2019, no. 1, pp. 68-83, Mar. 2019.
- [6] M. Salucci, G. Oliveri, N. Anselmi, and A. Massa, "Material-by-design synthesis of conformal miniaturized linear phased arrays," *IEEE Access*, vol. 6, pp. 26367-26382, 2018.
- [7] M. Salucci, G. Oliveri, N. Anselmi, G. Gottardi, and A. Massa, "Performance enhancement of linear active electronically-scanned arrays by means of MbD-synthesized metalenses," *Journal of Electromagnetic Waves and Applications*, vol. 32, no. 8, pp. 927-955, 2018.
- [8] G. Oliveri, M. Salucci, N. Anselmi and A. Massa, "Multiscale System-by-Design synthesis of printed WAIMs for waveguide array enhancement," *IEEE J. Multiscale Multiphysics Computat. Techn.*, vol. 2, pp. 84-96, 2017.
- [9] A. Massa and G. Oliveri, "Metamaterial-by-Design: Theory, methods, and applications to communications and sensing - Editorial," *EPJ Applied Metamaterials*, vol. 3, no. E1, pp. 1-3, 2016.
- [10] G. Oliveri, F. Viani, N. Anselmi, and A. Massa, "Synthesis of multi-layer WAIM coatings for planar phased arrays within the system-by-design framework," *IEEE Trans. Antennas Propag.*, vol. 63, no. 6, pp. 2482-2496, June 2015.
- [11] G. Oliveri, L. Tenuti, E. Bekele, M. Carlin, and A. Massa, "An SbD-QCTO approach to the synthesis of isotropic metamaterial lenses" *IEEE Antennas Wireless Propag. Lett.*, vol. 13, pp. 1783-1786, 2014.

-
- [12] A. Massa, G. Oliveri, P. Rocca, and F. Viani, "System-by-Design: a new paradigm for handling design complexity," *8th European Conference on Antennas Propag. (EuCAP 2014)*, The Hague, The Netherlands, pp. 1180-1183, Apr. 6-11, 2014.
- [13] P. Rocca, M. Benedetti, M. Donelli, D. Franceschini, and A. Massa, "Evolutionary optimization as applied to inverse problems," *Inverse Problems - 25 th Year Special Issue of Inverse Problems, Invited Topical Review*, vol. 25, pp. 1-41, Dec. 2009.
- [14] P. Rocca, G. Oliveri, and A. Massa, "Differential Evolution as applied to electromagnetics," *IEEE Antennas Propag. Mag.*, vol. 53, no. 1, pp. 38-49, Feb. 2011.
- [15] P. Rocca, N. Anselmi, A. Polo, and A. Massa, "Pareto-optimal domino-tiling of orthogonal polygon phased arrays," *IEEE Trans. Antennas Propag.*, vol. 70, no. 5, pp. 3329-3342, May 2022.
- [16] P. Rocca, N. Anselmi, A. Polo, and A. Massa, "An irregular two-sizes square tiling method for the design of isophoric phased arrays," *IEEE Trans. Antennas Propag.*, vol. 68, no. 6, pp. 4437-4449, Jun. 2020.
- [17] P. Rocca, N. Anselmi, A. Polo, and A. Massa, "Modular design of hexagonal phased arrays through diamond tiles," *IEEE Trans. Antennas Propag.*, vol. 68, no. 5, pp. 3598-3612, May 2020.
- [18] N. Anselmi, L. Poli, P. Rocca, and A. Massa, "Design of simplified array layouts for preliminary experimental testing and validation of large AESAs," *IEEE Trans. Antennas Propag.*, vol. 66, no. 12, pp. 6906-6920, Dec. 2018.
- [19] N. Anselmi, P. Rocca, M. Salucci, and A. Massa, "Contiguous phase-clustering in multibeam-on-receive scanning arrays" *IEEE Trans. Antennas Propag.*, vol. 66, no. 11, pp. 5879-5891, Nov. 2018.
- [20] G. Oliveri, G. Gottardi, F. Robol, A. Polo, L. Poli, M. Salucci, M. Chuan, C. Massagrande, P. Vinetti, M. Mattivi, R. Lombardi, and A. Massa, "Co-design of unconventional array architectures and antenna elements for 5G base station," *IEEE Trans. Antennas Propag.*, vol. 65, no. 12, pp. 6752-6767, Dec. 2017.
- [21] N. Anselmi, P. Rocca, M. Salucci, and A. Massa, "Irregular phased array tiling by means of analytic schemata-driven optimization," *IEEE Trans. Antennas Propag.*, vol. 65, no. 9, pp. 4495-4510, September 2017.
- [22] N. Anselmi, P. Rocca, M. Salucci, and A. Massa, "Optimization of excitation tolerances for robust beam-forming in linear arrays" *IET Microwaves, Antennas & Propagation*, vol. 10, no. 2, pp. 208-214, 2016.
- [23] P. Rocca, R. J. Mailloux, and G. Toso, "GA-Based optimization of irregular sub-array layouts for wideband phased arrays design," *IEEE Antennas and Wireless Propag. Lett.*, vol. 14, pp. 131-134, 2015.
- [24] P. Rocca, M. Donelli, G. Oliveri, F. Viani, and A. Massa, "Reconfigurable sum-difference pattern by means of parasitic elements for forward-looking monopulse radar," *IET Radar, Sonar & Navigation*, vol. 7, no. 7, pp. 747-754, 2013.

-
- [25] M. Salucci, L. Poli, A. F. Morabito, and P. Rocca, "Adaptive nulling through subarray switching in planar antenna arrays," *Journal of Electromagnetic Waves and Applications*, vol. 30, no. 3, pp. 404-414, February 2016
- [26] T. Moriyama, L. Poli, and P. Rocca, "Adaptive nulling in thinned planar arrays through genetic algorithms" *IEICE Electronics Express*, vol. 11, no. 21, pp. 1-9, Sep. 2014.
- [27] L. Poli, P. Rocca, M. Salucci, and A. Massa, "Reconfigurable thinning for the adaptive control of linear arrays," *IEEE Trans. Antennas Propag.*, vol. 61, no. 10, pp. 5068-5077, Oct. 2013.
- [28] P. Rocca, L. Poli, G. Oliveri, and A. Massa, "Adaptive nulling in time-varying scenarios through time-modulated linear arrays," *IEEE Antennas Wireless Propag. Lett.*, vol. 11, pp. 101-104, 2012.